KIMIKA Volume 19, Number 2, pp. 91–96 (2003)
© 2003 Kapisanang Kimika ng Pilipinas
All rights reserved. Printed in the Philippines
ISSN 0115–2130

Synthesis, characterization, molecular modelling studies of a novel liquid crystal for use in laser-addressed displays

Larry R. Manuel[1]*, Leonorina G. Cada[1], and Liang-chy Chien[2]

[1]*Institute of Chemistry*
University of the Philippines
Diliman, Quezon City
Metro Manila 1001, PHILIPPINES

[2]*Liquid Crystal Institute*
Kent State University
Kent, Ohio, USA

R-(+)- and S-(–)-2-octyl-[4"-decyloxy-3,3'-difluoro]-4-terphenylate (4-DDOT) were synthesized and characterized completely for possible use in laser- addressed displays. The pertinent structural features in this compound are the 3,3' positions of the lateral Fluorines in the ring and the respective donor- acceptor effect of the alkoxy terminal functionalities to extend aromatic conjugation [1]. A not so large Fluorine separation favors the formation of a Smectic A phase, the phase, which is desirable for the aforementioned type of displays [2].

Spectroscopic techniques such as ^{1}H NMR, ^{13}C NMR, and FTIR were employed for structural determination. DSC (for determination of transition temperatures), OPM and X-ray (for mesophase identification) measurements were also done. These compounds were also subjected for polarimetric measurements. Cambridge and ACD lab Software molecular modeling program were employed for structural determination and theoretical comparison.

Keywords: liquid crystals; difluorinated terphenyls; smectic phases

INTRODUCTION

Liquid crystals exhibiting the smectic A phase can be utilized as materials in projection display technology. Projection displays are effective means of displaying complex information to an audience [4]. The high contrast ratio needed for such displays can be achieved using a light scattering texture on a clear transparent background (normal mode), or vice versa (reverse mode) [5]. It has been found that such displays can be addressed by laser beams such as He-Ne, GaAs or GaAlAs [3].

The mode of operation (from off to on state) is shown schematically in Fig. 1. In here, the S_A liquid crystal (laser addressed or thermally addressed) such as DDOT is sandwiched between two glass plates, the inner surfaces of the glass being coated with a transparent conducting layer, usually indium tin oxide (ITO), then voltages were applied to effect the switching process. The glass plates' thickness may vary from 3–14 μm [3, 6].

**To whom correspondence should be addressed.*

With E-field **W/out E-field**

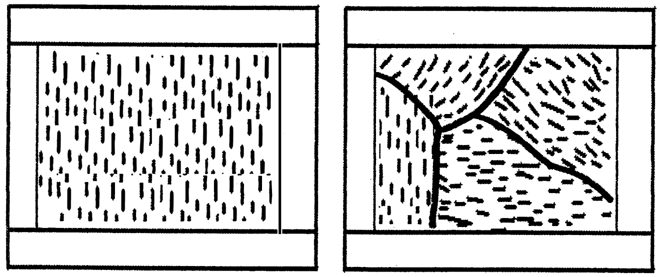

A B

Fig. 1. Smectic liquid crystal display. If cooled from the nematic phase in the presence of an electric field, the state shown in (A) *forms and is transparent. Cooling without an electric field produces the state shown in* (B) *which is highly scattering.*

Difluorinated terphenyls, which include DDOT, still are one of the best materials for display application, among similar fluorinated polyphenyl FLCs, because they exhibit relatively low transition temperatures. This can be explained mainly by three factors such as: broadening of the molecule, twisting about the inter-annular bond and position of the flourine atom on an outer or inner edge [2].

In this paper we present the synthesis, characterization and molecular modeling studies of a novel difluorinated terphenylate [1, 7–10].

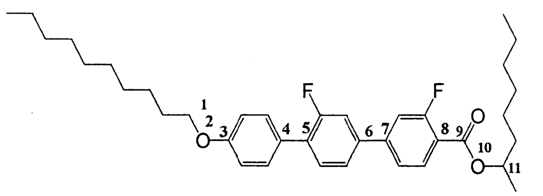

Fig. 2. R-(+)- and S-(-)-2-octyl-[4"-decyloxy-3-3'-difluro]-4-terphenylate (4-DDOT)

EXPERIMENTAL

Evaluation of features and physical properties were accomplished by employing several spectroscopic techniques. Structures and chemical purities were confirmed by ^{1}H and ^{13}C NMR spectra using a 200 MHz Varian- Gemini NMR spectrometer, with $CDCl_3$ as solvent (unless otherwise stated in the specific spectra) and TMS as internal standard; a Nicolet Magna-FTIR 550 Spectrophotometer and a Waters reversed-phase HPLC System 994 equipped with Waters 510 Solvent Delivery System, Waters U6K Universal Injector and Waters UV-Vis Spectrometer as detector. C-18 packing material was used. 60 CH_2Cl_2/40 MeOH was used as the mobile solvent mixture for the analysis. Flow rate is 1.00 mL/min and the flow cell is 10.00 mm. The column has an inner diameter of 3.9 mm and a length of 15.00 cm.

Optical rotations were determined by a Polyscience SR6 polarimeter using $CHCl_3$ as the solvent.

Mesomorphic properties such as textures and transition temperatures were determined by optical microscopy using a Leitz Laborlux S polarized microscope (magnification 200×) equipped with a Mettler FP52 hot stage, a Mettler FP5 control unit and a Wild Leitz MP552 camera in conjunction with Perkin-Elmer DSC 7 differential scanning calorimetry equipped with TAC7/DX thermal analysis controller. Heating and cooling scan rate of 1.0°C/min was used. Transition temperatures were reported as the maxima and minima of their endothermic and exothermic peaks, respectively.

The chemical structure of DDOT was drawn in CS Chem Draw Pro. It was then pasted on CS Chem 3D Pro. From the main menu of Chem 3D Pro, MM2 was selected, followed by the Minimize Energy command. The Run button in the minimize energy dialog box was clicked to begin minimization of the model. A particular minimized conformer along with pertinent measurements was obtained. The first trial served as the starting configuration. Bonds, labelled 1–2, 2–3, 4–5, 6–7, 8–9, 9–10, and 10–11 (refer to 4-DDOT) were rotated one at a time to

Table 1. Molecular modeling data of the most stable configuration of compound IG, using Cambridge Software 3D PRO.

Energy Breakdown of the Total Energy = 14.4270 kcal		
Stretch	2.5389	
Bend	6.6356	
Stretch-Bend	0.5241	
Torsion	–21.6898	
Non-1,4 VDW	–4.9041	
1,4 VDW	28.2546	
Dipole/Dipole	3.0676	
Selected Bond Distance and Torsion Angles		
Bond Distances, Å	Bond Distances, Å	Torsion angles, degree
C1-C2 = 1.397	C15-F32 = 1.322	C41-C40-C39-C38 = 179.684
C1-C6 = 1.399	C16-C17 = 1.402	C12-C11-O19-C42 = 3.953
C2-C3 = 1.4000	C16-C20 = 1.493	**C13-C8-C3-C4 = 45.750**
C2-H44 = 1.102	C17-C18 = 1.399	**C5-C6-C7-C18 = –42.757**
C3-C4 = 1.402	C17-H51 = 1.102	C17-C16-C20-O23 = –2.002
C3-C8 = 1.488	O19-C42 = 1.416	C16-C20-O24-C21 = –177
C4-C5 = 1.398	C20-O23 = 1.228	C33-C42-O19-C11 = 3.953
C4-F31 = 1.323	C20-O24 = 1.365	C25-C21-O24-C20 = 77.477
C5-C6 = 1.399	C21-C22 = 1.534	F31-C4-C3-C8 = 1.644
C6-C7 = 1.488	C21-O24 = 1.418	F31-C15-C16-C20 = 178.584
C7-C14 = 1.402	C21-C25 = 1.531	F32-C15-C16-C20 = 0.00
C7-C18 = 1.397	C29-C30 = 1.534	C32-C15-C14-C7 = 179.457
C8-C9 = 1.399	C33-C42 = 1.530	
C8-C13 = 1.398	C35-H74 = 1.116	
C9-C10 = 1.397	C38-C39 = 1.537	
C11-C12 = 1.402	C39-C40 = 1.537	
C11-O19 = 1.374	C40-C41 = 1.535	
C12-C13 = 1.397	C40-H84 = 1.116	
C14-C15 = 1.396	C41-H86 = 1.114	
C15-C16 = 1.407		

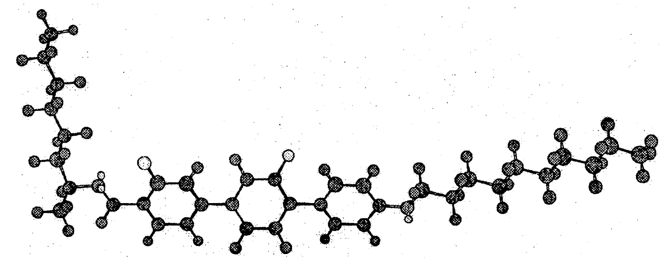

Fig. 3. Minimized energy configuration of IG compound.

Table 2. Molecular modeling data of the most stable configuration of the saturated Compound IG, using ACD 3D PRO.

Longest Distance H85–H63, approximate mol length	31.5558 Å
Distance between F31 and F32	7.2050 Å
Distance between C11 and C16	11.4963 Å
Distance between F31 and H85	18.8697 Å

Selected Bond Distance and Torsion Angles

Bond Distances, Å	Bond Distances, Å	Torsion angles, degree
C1-C2 = 1.3973	C15-F32 = 1.3222	C41-C40-C39-C38 = 179.709
C1-C6 = 1.3985	C16-C17 = 1.4024	C12-C11-O19-C42 = 173.908
C2-C3 = 1.4004	C16-C20 = 1.4931	**C13-C8-C3-C4 = 45.753**
C2-H44 = 1.1020	C17-C18 = 1.3986	**C5-C6-C7-C18 = –42.757**
C3-C4 = 1.4022	C17-H51 = 1.1016	C17-C16-C20-O23 = 1.996
C3-C8 = 1.4876	O19-C42 = 1.4163	C16-C20-O24-C21 = 177.332
C4-C5 = 1.3980	C20-O23 = 1.2275	C33-C42-O19-C11 = 175.832
C4-F31 = 1.3228	C20-O24 = 1.3646	C25-C21-O24-C20 = 77.476
C5-C6 = 1.3992	C21-C22 = 1.5339	F31-C4-C3-C8 = 1.645
C6-C7 = 1.4883	C21-O24 = 1.4180	F31-C15-C16-C20 = 178.583
C7-C14 = 1.407	C21-C25 = 1.5306	F32-C15-C16-C20 = 0.179
C7-C18 = 1.3972	C29-C30 = 1.5345	C32-C15-C14-C7 = 179.471
C8-C9 = 1.3991	C33-C42 = 1.5300	
C8-C13 = 1.3984	C35-H74 = 1.1161	
C9-C10 = 1.3968	C38-C39 = 1.5374	
C11-C12 = 1.4019	C39-C40 = 1.5371	
C11-O19 = 1.3736	C40-C41 = 1.5346	
C12-C13 = 1.3965	C40-H84 = 1.1163	
C14-C15 = 1.3956	C41-H86 = 1.140	
C15-C16 = 1.4069		

effect different configurations. They were rotated, with a degree rotation gradient, until a 360° rotation has been accomplished. These way at least 2000 rotations were accomplished, corresponding to the attainment of same number of conformers having minimum steric energies. The software is user- friendly in this regards just like in the energy minimization procedure. The conformer shown in Fig. 3 was chosen to be the most stable conformer out of these enormous data. It must be noted, however, that the absolute values of the steric energies obtained in these studies do not have any physical significance. Measurements were then recorded together with the minimized configuration (Table 1). The most stable MM2 configuration models were then imported to the ACD Lab Software individually. Two atoms were specified to measure bond lengths and bond distances; while three interconnected bonds (or four interconnected atoms) were highlighted, from the drawn model, for dihedral angle measurements. After these specifications, the Measure button was selected. Measurements were then displayed on screen and then recorded (Table 2).

RESULTS AND DISCUSSION

The 7-step synthesis of DDOT made use of the Williamson ether synthesis, BuLi reaction, Suzuki coupling, $KMnO_4$ oxidation esterification reactions (scheme 1). The overall yield for the 6-step linear synthesis is >9% with the last esterification step using the DEAD method having the lowest yield most probably due to solubility problems (see Figs. 3–5 for the NMR and IR of DDOT). The HPLC result shows a retention peak at 3.39 min while the $[\alpha]^{20} = +33°$.

DDOT showed only the textures of the S_A phase under OPM (Fig. 7–9), persisting till room temperature, if the sample is cooled from the isotropic phase. These three pictures comprise a series showing the changes in the crystallites when the temperature is increased from 40°C to 75°C then 80°C. The DSC heating curve shows the following temperature transitions:

K34.27 (70.16) S_A (or S_A*) 83.31(6.92) I.

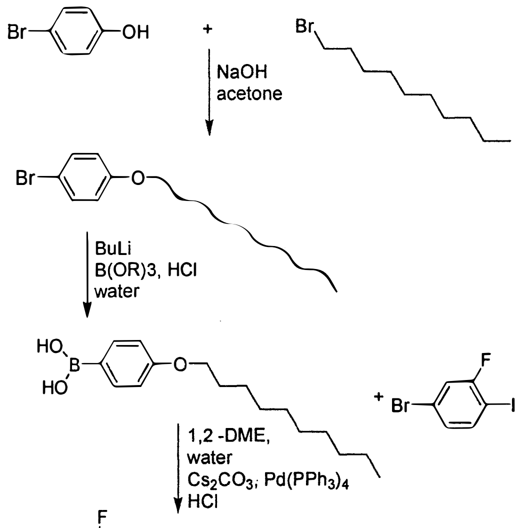

Scheme 1. Synthesis of R-(+) or S-(–)-2-octyl-[4"-decylocy-3,3'difluro]-4-terphenylate

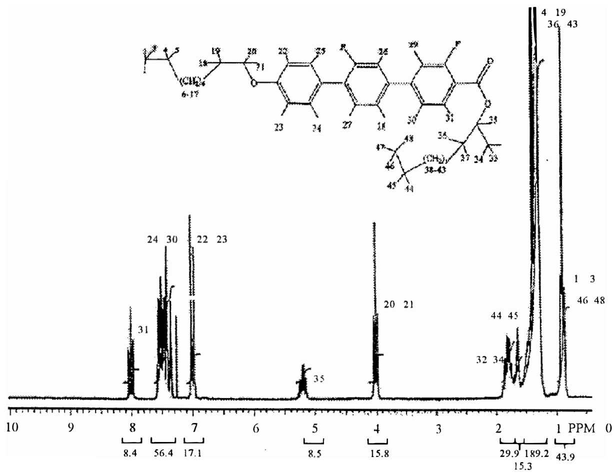

Fig. 4. Proton NMR of IG (isomeric product using R-(-)-2-octanol).

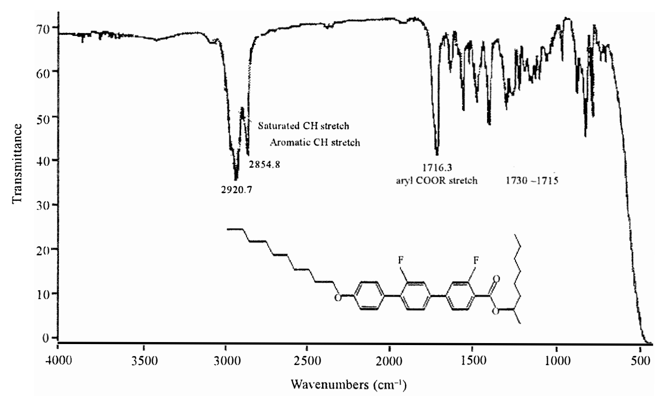

Fig. 5. IR of IG.

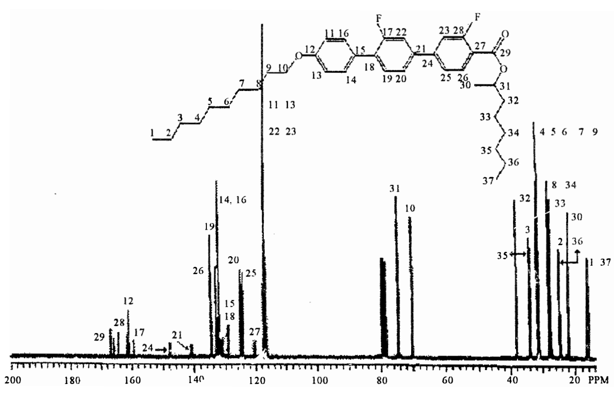

Fig. 6. Carbon-13 NMR of IG.

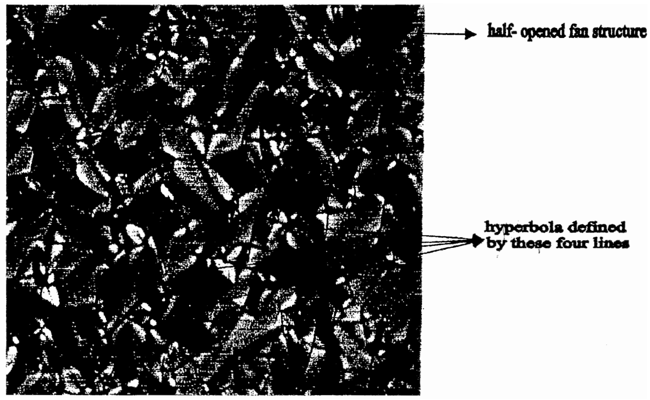

Fig. 7. Smectic A phase of Compound IG at 40 ℃ characterized by hyperbolas found in the fan shaped texture.

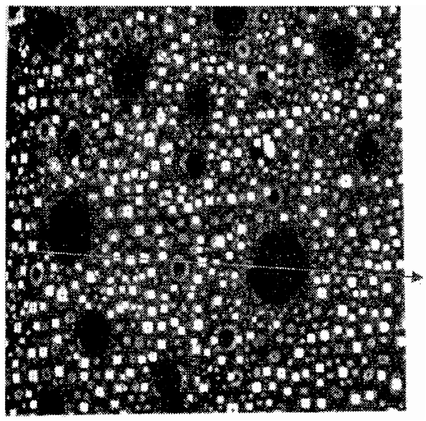

A Maltese cross which is a cylindrical Focal conic; of varied size; this rotates either clockwise or anticlockwise by the tilt angle.

Fig. 8. Bubble domains marked by Maltese crosses as observed under crossed polarizers in poorly aligned samples of compound IG (as the sample is being cooled at 80 ℃ from the isotropic state).

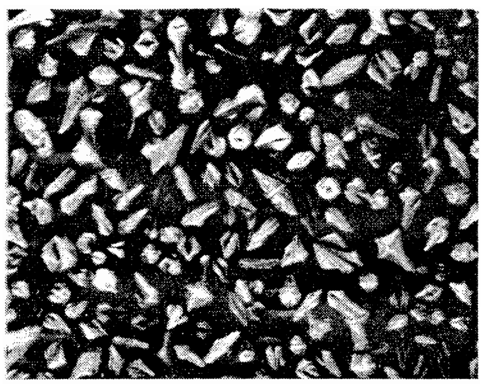

Fig. 9. Smectic A Crystallites at 75 ℃ of **IG** Compound.

The exothermic curve, on the other hand, has I83.07 (–4.64) SA (or S_A*). This curve also shows that DDOT supercools until –40°C (i.e., no melting point peak was observed) (Figs. 10 and 11).

The separation of lateral fluorine atoms according to ACD Lab Software is 7.2050 Å. This may not be big enough to induce tilting and thus prevented the formation of chiral smectic C phase and favor only the smectic A phase. The DSC and OPM experiments of DDOT showed only the latter phase. The X-ray

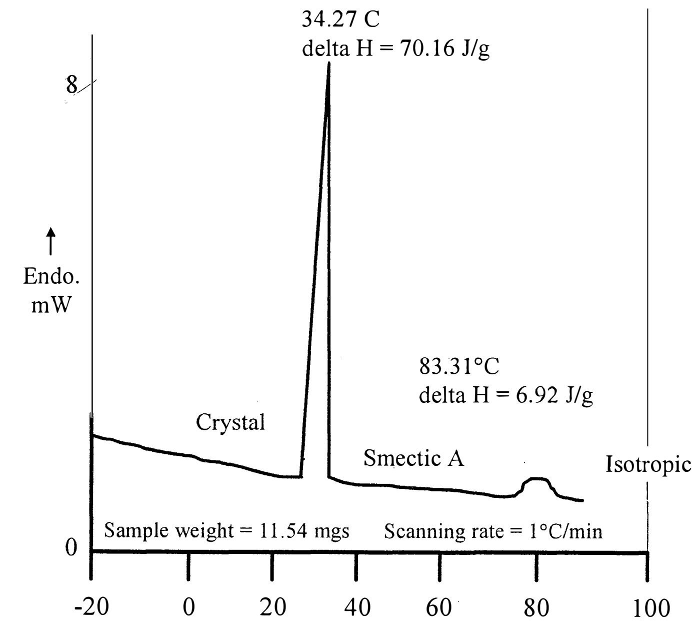

Fig. 10. DSC heating curve of IG compound.

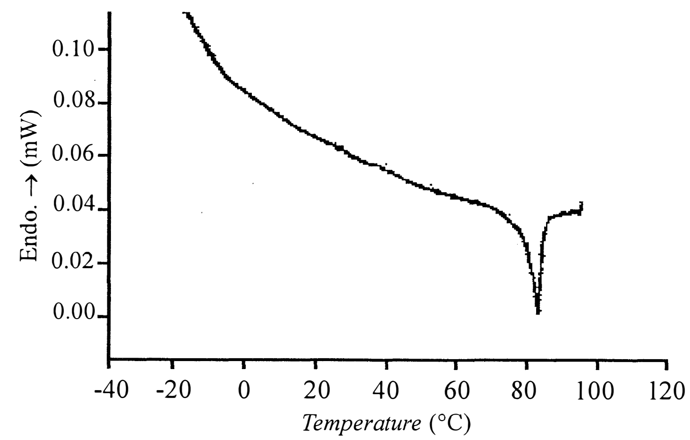

Fig. 11. DSC cooling curve of IG compound.

measurement (for d and θ determination) of which shows a broad reflection at wide angles (associated with the lateral packing) and a sharp reflection (Intensity = 42) at small angles (2θ = 2.10°, θ= 1.05°) (associated with the smectic layers) (Fig. 12).

Molecular modelling further revealed a value of 31.5558 Å for l (molecular length). In conjunction with the x-ray value of 42.00 Å for d, it can be surmised that this phase has a modulated structure because $l < d < 2l$, $d \approx 1.5l$]. It is now more aptly labelled as $S_{A,d}$ (Fig. 13).

From MM2/MOPAC calculations, DDOT has a minimized steric energy of 14.4270 ± 0.0197 kcal/mole or 14.43 ± 0.02; $\Delta H_f = -236.62$ kcal/mole and 3.0676 kcal/mole dipole- dipole energy contribution. (see Fig. 3). With this result of dipole-dipole energy calculations, one can conclude that the possibility

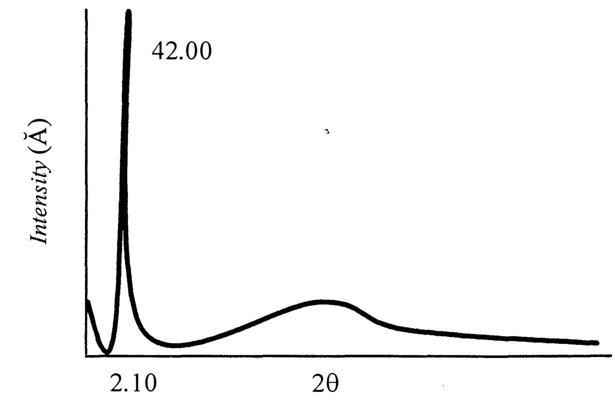

Fig. 12. Intensity vs. 2q spectra of the powder x-ray diffraction measurement of IG at 55°C.

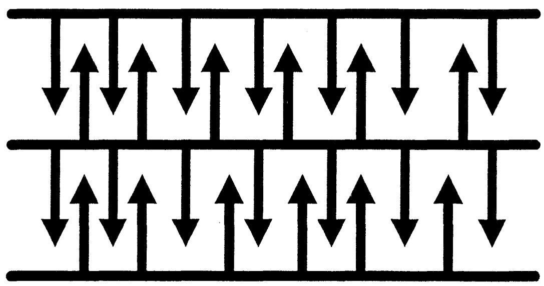

Fig. 13. Stick representation of the molecules in S_{Ad} phase. Arrows represent polar groups. This phase is usually composed of antiparallel dimers which are due to existence of permanent electric dipoles.

of cancellation of dipoles did not happen and therefore not responsible for the absence of S_C*. It may also be surmised that the dipole moment of this molecule will be towards the ester moiety with some degree of offset/tilt from the long molecular axis because of the presence of lateral fluorine atoms (the direction of this dipole may also be viewed along the short molecular axis with a little degree of tilt).

Polarimetric measurement showed $[\alpha]^{20} = +33$ maintaining the dextrorotatory property of the *S-(+)-2-octanol* employed. Since the DEAD esterification is known to lead to configuration inversion, the final configuration of the DDOT compound may be deduced to be R-(+).

ACKNOWLEDGMENT

We thank the DOST- ESEP for funding the experimental portion of this work. Mr. Manuel also would like to thank the Liquid Crystal Institute of Kent State University where most of the work was done specifically Drs. Liang-chy Chien, John West and Satyendra Kumar. Also the help of Mr. Eckart dela Cruz in finishing this manuscript is greatly appreciated.

REFERENCES

1. Liu and Nohira. *Liquid Crystals.* 20 (5), 581 (1996).

2. McDonnell, Sage, Hird, Toyne, and Gray. *Liquid Crystals.* 18 (1), 1 (1995).

3. Collings, P. J. *Liquid Crystals. Nature's Delicate Phase of Matter.* (Princeton University Press: New Jersey, 1990).

4. Bahadur, B. *Mol. Cryst. Liq. Cryst.* 109, 3 (1984).

5. Bahadur, B. *In* Bahadur, B. (Ed.) *Liquid Crystals. Applications and Uses,* Vol. 3, p. 4. (World Scientific: London, 1990).

6. Blinov, L. M. and Chigrinov, V.G. *Electrooptic Effects in Liquid Crystal Materials.* (Springer: New York, 1996).

7. Booth, D., Goodby, and Toyne. *Liquid Crystals.* 20 (6), 815 (1996).

8. Chan, Gray, and Lacey. *Mol. Cryst. Liq. Cryst.* 123, 185 (1985).

9. Glendenning, Goodby, Hird, Jones, Toyne, Slaney, and Minter. *Mol. Cryst. Liq. Cryst.* 332, 321 (1999).

10. Glendenning, Goodby, Hird, and Toyne. *J. Chem. Soc., Perkin. Trans.* 2, 481 (1999).